Training Sequence-aided QRM-MLD Block Signal Detection for Single-carrier MIMO Spatial Multiplexing

Tetsuya YAMAMOTO† Kazuki TAKEDA† and Fumiyuki ADACHI‡
Dept. of Electrical and Communication Engineering, Graduate School of Engineering, Tohoku University
6-6-05 Aza-Aoba, Aramaki, Aoba-ku, Sendai, 980-8579 Japan
†{yamamoto, kazuki}@mobile.ecei.tohoku.ac.jp, ‡adachi@ecei.tohoku.ac.jp

***Abstract*—We propose a maximum likelihood block signal detection using QR decomposition and M-algorithm (called QRM-MLBD) for training sequence-aided single-carrier (TA-SC) multi-input multi-output (MIMO) spatial multiplexing. QRM-MLBD can significantly improve the packet error rate (PER) performance of cyclic prefix-inserted single-carrier (CP-SC) MIMO spatial multiplexing when compared to the frequency-domain minimum mean square error (MMSE) detection. However, in order to achieve the sufficiently improved performance, the use of a fairly large number *M* of surviving paths in the M-algorithm is required because if smaller *M* is used, the probability of removing the correct path at early stages increases. In this paper, to reduce this probability, we propose the use of TA-SC transmission instead of CP-SC transmission and show that the use of training sequence can significantly reduce the probability of removing the correct path at early stages in QRM-MLBD. We show, by computer simulation, that TA-SC MIMO spatial multiplexing using QRM-MLBD can achieve the PER performance similar to CP-SC MIMO spatial multiplexing while significantly reducing the computational complexity, about 8% of computational complexity of CP-SC MIMO in the case of 16QAM and 4×4 MIMO spatial multiplexing.**

Keywords-component; Single-carrier, MIMO, QRM-MLD, training sequence

I. INTRODUCTION

In next generation mobile communication systems, high data rate wireless communication systems are demanded. Multi-input multi-output (MIMO) spatial multiplexing [1] technique has been gaining much attention in a band-limited wireless channel. However, since the mobile wireless channel is composed of many propagation paths with different time delays, the channel becomes severely frequency-selective as the transmission data rate increases [2]. MIMO spatial multiplexing with orthogonal frequency-division multiplexing (OFDM) [3] is attractive. However, OFDM suffers from high peak-to-average power ratio (PAPR). Recently, MIMO spatial multiplexing with cyclic prefix-inserted single-carrier (CP-SC) block transmission using frequency-domain signal detection technique has been gaining an increasing popularity because of its lower PAPR property [4-5]. The use of CP and frequency-domain signal detection such as frequency-domain minimum mean square error (MMSE) detection [4] can improve the transmission performance of SC-MIMO spatial multiplexing with a low complexity. However, a big performance gap from the maximum likelihood (ML) performance still exists due to the presence of residual inter-symbol interference and inter-antenna interference.

The ML detection (MLD) [6] is the optimal detection scheme in terms of transmission performance. However, its computational complexity becomes extremely high because the number of symbol candidate sequence is exponentially increased to $X^{N_tN_c}$ for X-QAM, where N_t is the number of transmit antennas and N_c is the block size. Recently, near ML-based reduced complexity signal detection has been proposed in [7] for CP-SC MIMO spatial multiplexing (we call this detection scheme the ML block signal detection using QR decomposition and M-algorithm (QRM-MLBD)). In QRM-MLBD, QR decomposition is applied to a concatenation of the space and frequency-domain channel and discrete Fourier transform (DFT). It was shown [7] that QRM-MLBD can significantly improve the packet error rate (PER) performance of CP-SC MIMO spatial multiplexing when compared to the MMSE detection. However, in order to achieve the sufficiently improved performance, the use of a fairly large number *M* of surviving paths in the M-algorithm is required, leading to high computational complexity. This is because if smaller *M* is used, the probability of removing the correct path at early stages increases. Although [7] proposed the ordering method to solve this problem, a fairly large *M* must still be used to achieve the sufficiently improved PER performance.

In this paper, in order to further reduce the required number *M* of surviving paths for achieving the sufficiently improved PER performance, we propose a training sequence-aided QRM-MLBD for SC-MIMO spatial multiplexing. We previously showed [8] that the use of training sequence-aided SC (TA-SC) block transmission [9, 10] instead of CP-SC block transmission can significantly reduce the probability of removing the correct path at early stages in QRM-MLBD in the case of single-input single-output (SISO) case. We apply previously proposed training sequence-aided QRM-MLBD to the SC-MIMO spatial multiplexing. In the case of TA-SC MIMO spatial multiplexing, since the symbols to be detected at early stages belong to the known training sequences (TSs), the probability of removing the correct path at early stages can be significantly reduced.

The remainder of this paper is organized as follows. In Sect. II, TA-SC MIMO spatial multiplexing using QRM-MLBD is presented. In Sect. III, we will show some simulation results. We will also discuss the computational complexity of QRM-MLBD and show that TA-SC MIMO spatial multiplexing can reduce the overall complexity of QRM-MLBD to achieve almost the same performance as CP-SC MIMO spatial multiplexing. Sect. IV offers some concluding remarks.

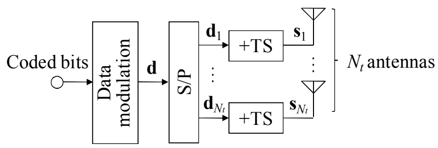

(a) Transmitter

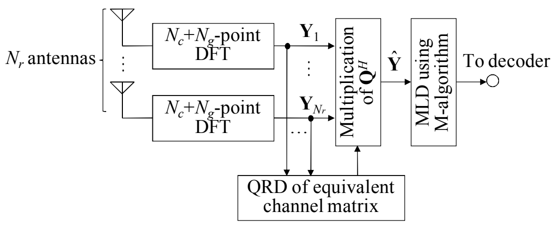

(b) Receiver

Figure 1. TA-SC MIMO multiplexing transmission system model.

II. TA-SC MIMO Spatial Multiplexing Using QRM-MLBD

A. Signal Transmission Model

TA-SC MIMO spatial multiplexing transmission model using QRM-MLBD is illustrated in Fig. 1. Throughout the paper, the symbol-spaced discrete time representation is used. At the transmitter, the data-modulated symbol sequence is serial-to-parallel (S/P) converted to N_t parallel symbol sequence, each to be transmitted from a different transmit antenna. The data symbol block of n_tth transmit antenna can be expressed using the vector form as $\mathbf{d}_{n_t} = [d_{n_t}(0),...,d_{n_t}(t),...,d_{n_t}(N_c-1)]^T$, where $(.)^T$ expresses the transposition. Before the transmission, the TS of length N_g symbols is appended at the end of each block. The block $\mathbf{s}_{n_t} = [s_{n_t}(0),...,s_{n_t}(t),...,s_{n_t}(N_c+N_g-1)]^T$ to be transmitted is expressed using the vector form as

$$\begin{aligned}\mathbf{s}_{n_t} &= [d_{n_t}(0),...,d_{n_t}(N_c-1),u_{n_t}(0),...,u_{n_t}(N_g-1)]^T \\ &= [\{\mathbf{d}_{n_t}\}^T \quad \{\mathbf{u}_{n_t}\}^T]^T\end{aligned}, \quad (1)$$

where $\mathbf{u}_{n_t} = [u_{n_t}(0),...,u_{n_t}(t),...,u_{n_t}(N_g-1)]^T$ denotes the TS vector which is identical for all blocks. The TA-SC block structure is illustrated and compared to CP-SC transmission in Fig. 2. The difference from CP-SC transmission is that CP is replaced by TS. In order to let TS to play the role of CP, DFT size at the receiver must be the sum of number of useful data symbols and the TS length. In this paper, to keep the same data rate as CP-SC, the data symbol block length and the TS length need to be set to N_c and N_g, respectively. Therefore, the DFT size to be used at the receiver is N_c+N_g symbols for TA-SC while it is N_c symbols for CP-SC. TA-SC requires slightly longer coherence time compared to that required by CP-SC due to the bigger DFT.

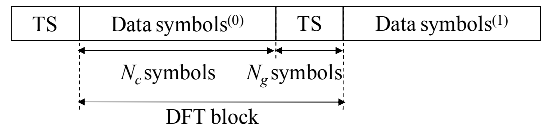

(a) TA-SC.

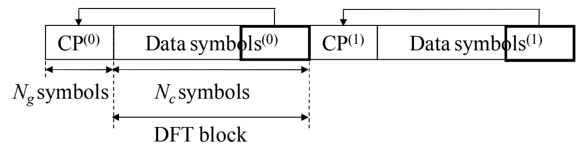

(b) CP-SC.

Figure 2. Block structure.

We assume a symbol-spaced frequency-selective fading channel composed of L propagation paths with different time delays. The channel impulse response between the n_tth transmit antenna and the n_rth receive antenna $h_{n_r,n_t}(\tau)$ is given by

$$h_{n_r,n_t}(\tau) = \sum_{l=0}^{L-1} h_{l,n_r,n_t}\delta(\tau-\tau_l), \quad (2)$$

where h_{l,n_r,n_t} and τ_l are respectively the complex-valued path gain with $E[\sum_{l=0}^{L-1}|h_{l,n_r,n_t}|^2]=1$ and the time delay of the lth path. The lth path time delay is assumed to be l symbols, i.e. τ_l=l.

Since the identical TS is used for all blocks, if we assume that $L \leq N_g$, the theorem of circular convolution is fulfilled. Therefore, the received signal block on the n_rth receive antenna $\mathbf{y}_{n_r} = [y_{n_r}(0),...,y_{n_r}(t),...,y_{n_r}(N_c+N_g-1)]^T$ can be expressed, similar to CP-SC transmission, as

$$\mathbf{y}_{n_r} = \sqrt{2E_s/T_s}\sum_{n_t=1}^{N_t}\mathbf{h}_{n_r,n_t}\mathbf{s}_{n_t} + \mathbf{n}_{n_r}, \quad (3)$$

where E_s and T_s are respectively the symbol energy and duration and $\mathbf{n}_{n_r} = [n_{n_r}(0),...,n_{n_r}(t),...,n_{n_r}(N_c+N_g-1)]^T$ is the noise vector. The tth element of $\mathbf{n}_{n_r}$ is the zero-mean additive white Gaussian noise (AWGN) having the variance $2N_0/T_s$ with N_0 being the one-sided noise power spectrum density. $\mathbf{h}_{n_r,n_t}$ is the $(N_c+N_g)\times(N_c+N_g)$ channel impulse response matrix between the n_tth transmit antenna and n_rth receive antenna, given as

$$\mathbf{h}_{n_r,n_t} = \begin{bmatrix} h_{0,n_r,n_t} & & & & h_{L-1,n_r,n_t} & & h_{1,n_r,n_t} \\ h_{1,n_r,n_t} & h_{0,n_r,n_t} & & & & \ddots & \vdots \\ \vdots & h_{1,n_r,n_t} & h_{0,n_r,n_t} & & \mathbf{0} & & h_{L-1,n_r,n_t} \\ h_{L-1,n_r,n_t} & \vdots & h_{1,n_r,n_t} & \ddots & & & \\ & h_{L-1,n_r,n_t} & \vdots & & h_{0,n_r,n_t} & & \\ & & h_{L-1,n_r,n_t} & & h_{1,n_r,n_t} & \ddots & \\ \mathbf{0} & & & \ddots & \vdots & & h_{0,n_r,n_t} \end{bmatrix}. \quad (4)$$

At the receiver, (N_c+N_g)-point DFT is applied to transform the received signal block into the frequency-domain signal vector $\mathbf{Y}_{n_r}=[Y_{n_r}(0),...,Y_{n_r}(k),...,Y_{n_r}(N_c+N_g-1)]^T$. $\mathbf{Y}_{n_r}$ is expressed as

$$\begin{aligned}\mathbf{Y}_{n_r}&=\mathbf{F}^{(N_c+N_g)}\mathbf{y}_{n_r}\\&=\sqrt{2E_s/T_s}\sum_{n_t=1}^{N_t}\mathbf{F}^{(N_c+N_g)}\mathbf{h}_{n_r,n_t}\mathbf{s}_{n_t}+\mathbf{F}^{(N_c+N_g)}\mathbf{n}_{n_r}\ ,\\&=\sqrt{2E_s/T_s}\sum_{n_t=1}^{N_t}\mathbf{H}_{n_r,n_t}\mathbf{F}^{(N_c+N_g)}\mathbf{s}_{n_t}+\mathbf{N}_{n_r}\end{aligned} \quad (5)$$

where $\mathbf{F}^{(J)}$ is the DFT matrix of size $J\times J$, given as

$$\mathbf{F}^{(J)}=\frac{1}{\sqrt{J}}\begin{bmatrix}1 & 1 & \cdots & 1\\ 1 & e^{-j2\pi\frac{1\times1}{J}} & \cdots & e^{-j2\pi\frac{1\times(J-1)}{J}}\\ \vdots & \vdots & \ddots & \vdots\\ 1 & e^{-j2\pi\frac{(J-1)\times1}{J}} & \cdots & e^{-j2\pi\frac{(J-1)\times(J-1)}{J}}\end{bmatrix} \quad (6)$$

and $\mathbf{N}_{n_r}=[N_{n_r}(0),...,N_{n_r}(k),...,N_{n_r}(N_c+N_g-1)]^T$ is the frequency-domain noise vector. The third line in Eq. (6) can be obtained by using the circulant property of $\mathbf{h}_{n_r,n_t}$, given as [11]

$$\begin{aligned}&\mathbf{F}^{(J)}\mathbf{h}_{n_r,n_t}\mathbf{F}^{(J)H}\\&=diag[H_{n_r,n_t}(0),\ldots,H_{n_r,n_t}(k),...,H_{n_r,n_t}(J-1)]\equiv\mathbf{H}_{n_r,n_t}\end{aligned}\ , \quad (7)$$

where $H_{n_r,n_t}(k)=\sum_{l=0}^{L-1}h_{l,n_r,n_t}\exp(-j2\pi k\tau_l/J)$, $k=0,1,...,J-1$, and $(.)^H$ is the Hermitian transpose.

B. QRM-MLBD

From Eq. (5), the $N_r(N_c+N_g)\times1$ overall frequency-domain received signal $\mathbf{Y}$ is given by [7] (in the following, the index (J) is omitted for simplicity)

$$\begin{aligned}\mathbf{Y}&=[\{\mathbf{Y}_1\}^T\ \cdots\ \{\mathbf{Y}_{N_r}\}^T]^T\\&=\sqrt{\frac{2E_s}{T_s}}\begin{bmatrix}\mathbf{H}_{1,1}\mathbf{F} & \mathbf{H}_{1,2}\mathbf{F} & \cdots & \mathbf{H}_{1,N_t}\mathbf{F}\\ \mathbf{H}_{2,1}\mathbf{F} & \mathbf{H}_{2,2}\mathbf{F} & \cdots & \mathbf{H}_{2,N_t}\mathbf{F}\\ \vdots & \vdots & \ddots & \vdots\\ \mathbf{H}_{N_r,1}\mathbf{F} & \mathbf{H}_{N_r,2}\mathbf{F} & \cdots & \mathbf{H}_{N_r,N_t}\mathbf{F}\end{bmatrix}\begin{bmatrix}\mathbf{s}_1\\ \vdots\\ \mathbf{s}_{N_t}\end{bmatrix}+\begin{bmatrix}\mathbf{N}_1\\ \vdots\\ \mathbf{N}_{N_r}\end{bmatrix},\\&=\sqrt{\frac{2E_s}{T_s}}\mathbf{H}\begin{bmatrix}\mathbf{s}_1\\ \vdots\\ \mathbf{s}_{N_t}\end{bmatrix}+\mathbf{N}\end{aligned} \quad (8)$$

where $\mathbf{H}$ is an equivalent channel matrix of size $N_r(N_c+N_g)\times N_t(N_c+N_g)$. QRM-MLBD can be applied to the SC-MIMO spatial multiplexing by treating a concatenation of the space and frequency-domain channel and DFT as this equivalent channel.

Identify applicable sponsor/s here. *(sponsors)*

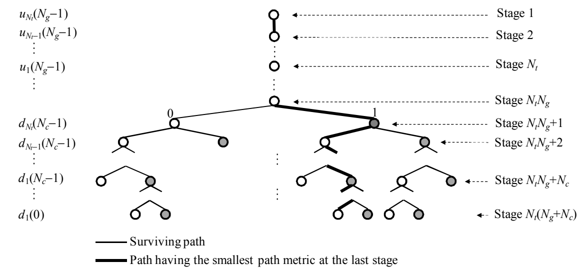

Figure 3. MLD using M-algorithm (M=3) with BPSK.

In [7], two ordering methods (antenna-first ordering and code-first ordering) were proposed for QRM-MLBD and [7] showed that code-first ordering significantly improves the PER performance than antenna-first ordering. Furthermore, in TA-SC MIMO multiplexing, by using code-first ordering, the TSs of all transmit antennas are focused in the bottom of transmit symbol vector. This property can be of considerable help in the MLD using M-algorithm. The symbols to be detected at early stages in M-algorithm belong to the known TSs, and therefore, the probability of removing the correct path can be significantly reduced. The transmit symbol vector $\mathbf{s}^{order}$ after code-first ordering can be expressed as

$$\begin{aligned}\mathbf{s}^{order}&=[s_1(0),...,s_{N_t}(0),...,s_1(N_c+N_g-1),...,s_{N_t}(N_c+N_g-1)]^T\\&=[\mathbf{d}^T(0),\mathbf{d}^T(1),...,\mathbf{d}^T(N_c-1),\mathbf{u}^T(0),...,\mathbf{u}^T(N_g-1)]^T\end{aligned}\ , \quad (9)$$

where $\mathbf{d}^T(t)$ and $\mathbf{u}^T(t)$ denote the data symbol vector and TS vector at tth symbol of size $N_t\times1$, respectively.

After ordering, the QR decomposition is applied to the ordered equivalent channel matrix $\mathbf{H}$ to obtain $\mathbf{H}=\mathbf{QR}$, where $\mathbf{Q}$ is an $N_r(N_c+N_g)\times N_t(N_c+N_g)$ matrix satisfying $\mathbf{Q}^H\mathbf{Q}=\mathbf{I}$ ($\mathbf{I}$ is an identity matrix) and $\mathbf{R}$ is an $N_t(N_c+N_g)\times N_t(N_c+N_g)$ upper triangular matrix. The transformed frequency-domain received signal $\hat{\mathbf{Y}}=[\hat{Y}(0),...,\hat{Y}(n),...,\hat{Y}(N_t(N_c+N_g)-1)]^T$ is obtained as

$$\hat{\mathbf{Y}}=\mathbf{Q}^H\mathbf{Y}=\sqrt{2E_s/T_s}\mathbf{R}\mathbf{s}^{order}+\mathbf{Q}^H\mathbf{N}\ . \quad (10)$$

From Eq. (10), the ML solution can be obtained by searching for the best path having the minimum Euclidean distance in the tree diagram composed of $N_t(N_c+N_g)$ stages. However, it can be understood from Eqs. (9) and (10) that in TA-SC MIMO multiplexing with code-first ordering, the $N_tN_c+1,N_tN_c+2,...,N_t(N_c+N_g)$th elements of $\hat{\mathbf{Y}}$ contain the training symbols only and therefore, only one path exists at the $n=1,2,...,N_tN_g$th stages as shown in Fig. 3, and therefore, the M-algorithm [12] can be started from the $n=N_tN_g+1$ stage. In each stage, the best M paths are selected as surviving paths by comparing the path metrics based on the squared Euclidean distance for all surviving paths and are passed to the next stage.

In the case of uncoded transmission, the data demodulation is carried out by tracing back the path having the smallest path metric at the last stage. On the other hand, in the case of coded transmission, the log likelihood ratio (LLR) is used as the soft-input in the decoder. When QRM-MLBD is used, however, the LLR values cannot be directly computed since surviving paths at the last stage do not necessarily contain both 1 and 0 for every coded bit. In this paper, we apply the LLR estimation method proposed in [13]. The approximate LLR values are computed at every stage by using path metric and are updated successively as tree search progresses. If the LLR value cannot be computed at the last stage, the recently updated approximate LLR value at the upper stage is used.

TABLE I. COMPUTER SIMULATION CONDITION

Transmitter	Channel code	Turbo code (R=3/4, 1)
	Data modulation	16QAM
	Number of transmit antennas	N_t=4
	Data symbol block length	N_c=64
	TS or CP lengths	N_g=16
Channel	Fading type	Frequency-selective block Rayleigh
	Power delay profile	L=16 path exponential power delay profile
	Decay factor	α=3dB
	Time delay	$\tau_l=l$ (l=0~L−1)
Receiver	Number of receive antennas	N_r=4
	Channel estimation	Ideal

III. COMPUTER SIMULATION

The average PER performance of 4×4 TA-SC MIMO spatial multiplexing using QRM-MLBD is evaluated by computer simulation and compared to CP-SC. The simulation condition is summarized in Table I. 16QAM is assumed as the data modulation scheme. We employ a rate 1/3 turbo encoder using two (13, 15) recursive systematic convolutional (RSC) component encoders. The two parity sequences from the turbo encoder are punctured to obtain rate-3/4 turbo codes. Log-MAP decoding with 6 iterations is assumed. The length of the information bit sequence is 3066. The data symbol block length is N_c=64 for both TA- and CP-SC and the TS length of TA-SC is N_g=16 which is equal to the CP length of CP-SC. A partial sequence taken from a PN sequence with a repetition period of 4095 bits is used as TS. The same data modulation is used for TS and useful data. The channel is assumed to be a frequency-selective block Rayleigh fading channel having symbol-spaced 16-path exponential power delay profile with decay factor 3dB. Ideal channel estimation is assumed.

A. *Average PER Performance*

The PER performance of uncoded TA-SC MIMO spatial multiplexing using QRM-MLBD is plotted in Fig. 4 as a function of average received symbol energy-to-noise power spectrum density ratio E_s/N_0 for M=1, 4, 16, 64, and 256. For comparison, the PER performance of CP-SC and the ML performance are also plotted (Since it is difficult to simulate the full MLD, we use the matched filter bound of 4 branch diversity [14] as ML performance). It can be seen form Fig. 4 that when small M is used, the achievable PER performance of CP-SC MIMO spatial multiplexing with QRM-MLBD degrades. On the other hand, TA-SC MIMO spatial multiplexing with QRM-MLBD can achieve better PER performance even if small M is used. TA-SC requires M=16 to achieve the PER performance similar to CP-SC with M=1024. Hence, TA-SC MIMO spatial multiplexing can reduce significantly the computational complexity required for the squared Euclidean distance calculations. Computational complexity reduction is discussed in Sect. III-B.

The PER performance of rate R=3/4 turbo coded TA-SC MIMO spatial multiplexing using QRM-MLBD is plotted in Fig. 5 as a function of average received E_s/N_0 for M=1, 4, 16, 64, and 256. For comparison, the PER performance of CP-SC is also plotted. It can be seen form Fig. 5 that as is the case in uncoded transmission, TA-SC can achieve better PER performance even if small M is used. The required value of M is 16 for TA-SC to achieve the PER performance similar to CP-SC using M=1024.

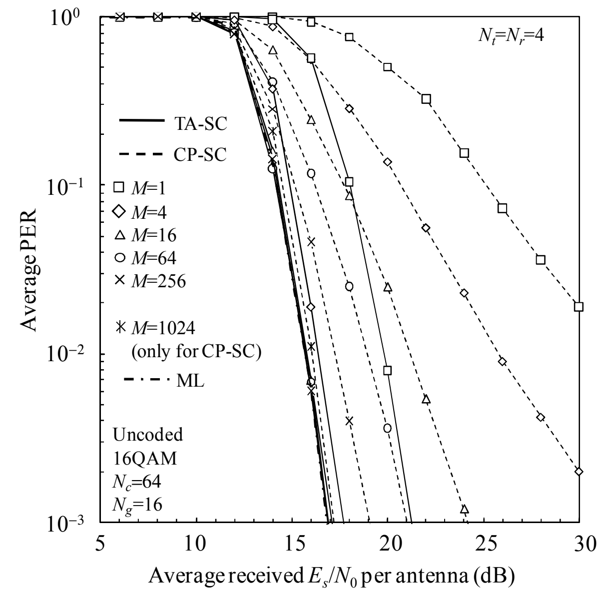

Figure 4. Average PER performance (uncoded). N_t=N_r=4.

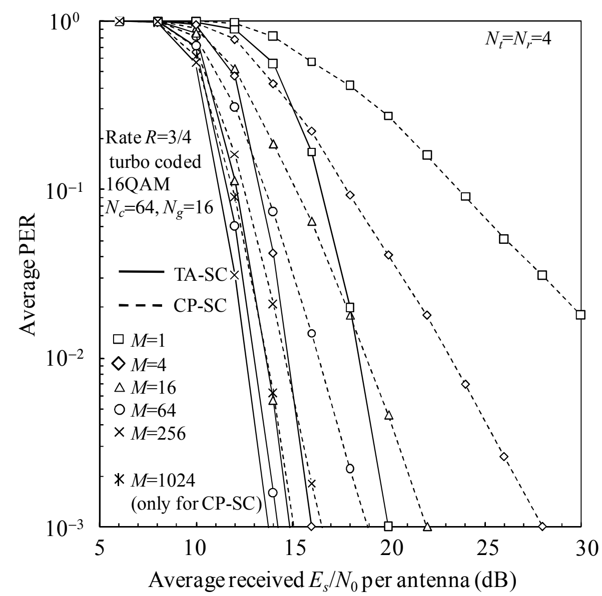

Figure 5. Average PER performance (rate R=3/4 turbo coded). N_t=N_r=4.

B. Computational Complexity

Below, we will discuss the overall computational complexity, which is the sum of the complexities required for DFT, equivalent channel matrix generation, QR decomposition, $\mathbf{Q}^H$ multiplication, and squared Euclidean distance calculation. The complexity here is defined as the number of complex-valued multiply operations. The required number of multiplications per block is shown in Table II. In TA-SC MIMO spatial multiplexing, DFT requires $N_r(N_c+N_g)^2$ multiplications. As a result, it requires large size of equivalent channel matrix $\mathbf{H}$ than that of CP-SC MIMO spatial multiplexing (resulting in higher complexity for equivalent channel matrix generation, QR decomposition, and multiplication of $\mathbf{Q}^H$). However, as discussed in Sect. III-A, TA-SC MIMO spatial multiplexing can reduce significantly the computational complexity required for the squared Euclidean distance calculations. As a result, the overall computational complexity for TA-SC MIMO spatial multiplexing is smaller than that of CP-SC MIMO spatial multiplexing. The overall computational complexity in TA-SC MIMO spatial multiplexing is about 8.2% of that in CP-SC MIMO spatial multiplexing for 16QAM in both uncoded and rate R=3/4 turbo coded case (Since the LLR estimation method [13] used in this paper can reuse the path metrics already calculated in MLD using M-algorithm, the computational complexity required for the QRM-MLBD for uncoded transmission and coded transmission is almost the same except for the complexity required for the turbo decoding).

TABLE II. NUMBER OF MULTIPLICATIONS PER BLOCK

	TA-SC MIMO	CP-SC MIMO
DFT	$N_r(N_c+N_g)^2$	$N_rN_c^2$
Equivalent channel matrix generation	$N_tN_r(N_c+N_g)^2$	$N_tN_rN_c^2$
QR decomposition [15]	$N_tN_r^2(N_c+N_g)^3$	$N_tN_r^2N_c^3$
Multiplication of $\mathbf{Q}^H$	$N_tN_r(N_c+N_g)^2$	$N_tN_rN_c^2$
Squared Euclidian distance calculations	$32+16N_tN_g$ $+16M\sum_{n=1}^{N_tN_c-1}(n+N_tN_g+2)$	$32+16M\sum_{n=1}^{N_tN_c-1}(n+2)$
Total complexity (N_t=N_r=4, N_c=64, and N_g=16)	4.6×10^7	5.6×10^8

IV. CONCLUSION

In this paper, we proposed a training sequence-aided QRM-MLBD for SC-MIMO spatial multiplexing. In the case of TA-SC MIMO spatial multiplexing, since the symbols to be detected at early stages belong to the known TSs, the probability of removing the correct path at early stages can be significantly reduced. We showed by computer simulation that training sequence-aided QRM-MLBD for TA-SC MIMO spatial multiplexing can achieve the PER performance similar CP-SC while reducing the number of surviving paths. In both uncoded and coded case, the required value of M in TA-SC MIMO spatial multiplexing is 16 to achieve the PER performance similar to CP-SC MIMO spatial multiplexing using M=1024. Therefore, the computational complexity required for QRM-MLBD is greatly reduced. The overall complexity required for QRM-MLBD in TA-SC MIMO spatial multiplexing is reduced to about 8.1% of that in CP-SC MIMO spatial multiplexing for 16QAM, N_t=N_r=4, N_c=64, and N_g=16.

REFERENCES

[1] G. J. Foschini and M. J. Gans, "On limit of wireless communications ini a fading environment when using multiple antennas," Wireless Personal Commun., Vol. 6, No. 3, pp. 311-335, 1998.

[2] J. G. Proakis and M. Salehi, *Digital communications*, 5th ed., McGraw-Hill, 2008.

[3] K. Higuchi, H. Kawai, N. Maeda, H. Taoka, and M, Sawahashi, "Experiments on real-time 1-Gb/s packet transmission using MLD-based signal detection in MIMO-OFDM broadband radio access," IEEE Journal on Selected Areas in Commun., Vol. 24, No. 6, pp. 1141-1153, June 2006.

[4] A. Nakajima, D. Garg, and F. Adachi, "Throughput of turbo coded hybrid ARQ using single-carrier MIMO multiplexing," in Proc. IEEE 61st Vehicular Technology Conference (VTC2005-Spring), Vol. 1, pp. 610-614, 30 May-1 June 2005.

[5] N. Benjamin, L. Chan-Tong, and D. Falconer, "Trubo frequency domain equalization for single-carrier broadband wireless systems," IEEE Trans. on Wireless Commun., Vol. 6, No. 2, pp. 759-767, Feb. 2007.

[6] A. van Zelst, R. van Nee, and G. A. Awater, "Space division multiplexing (SDM) for OFDM systems," in Proc. IEEE 51st Vehicular Technology Conference (VTC2000-Spring), Vol. 2, pp. 1070-1074, May 2000.

[7] K. Nagatomi, K. Higuchi, and H. Kawai, "Complexity reduced MLD based on QR decomposition in OFDM MIMO multiplexing with frequency domain spreading and code multiplexing," in Proc. IEEE Wireless Communications and Networking Conference (WCNC 2009), pp. 1-6, Apr. 2009.

[8] T. Yamamoto, K. Takeda, and F. Adachi, "Training sequence-aided single-carrier block signal detection using QRM-MLD," in Proc. IEEE Wireless Communications and Networking Conference (WCNC 2010), pp. 1-6, Apr. 2010.

[9] L. Deneire, B. Gyselinckx, and M. Engels, "Training sequence versus cyclic prefix - a new look on single carrier communication," IEEE Commun. Lett., Vol. 5, No. 7, pp. 292-294, July, 2001.

[10] J. Coon, M. Sandell, M. Beach, and J. McGeehan, "Channel and noise variance estimation and tracking algorithms for unique-word based single-carrier systems," IEEE Trans. on Wireless Commun., Vol. 5, No. 6, pp. 1488-1496, June 2006.

[11] G. H. Golub and C. F. van Loan, *Matrix Computations*, 3rd ed. Baltimore, MD, Johns Hopkins Univ. Press, 1996.

[12] J. B. Anderson and S. Mohan, "Sequential coding algo-rithms: A survey and cost analysis," IEEE Trans. on Commun., Vol. 32, No. 2, pp. 169-176, Feb. 1984.

[13] W. Shin, H. Kim, M Son, and H. Park, "An improved LLR computation for QRM-MLD in coded MIMO systems," in Proc. IEEE 66th Vehicular Technol-ogy Conference (VTC2007-Fall), pp.447-451, 30 Sept.-3 Oct. 2007.

[14] F. Adachi and K. Takeda, "Bit error rate analysis of DS-CDMA with joint frequency-domain equalization and an-tenna diversity combining," IEICE Trans. Commun., Vol. E87-B, No. 10, pp.2991-3002, Oct. 2004.

[15] D. Morale-Jimenez, J. F. Paris, and, J. T. Entrambasaguas, "Performance tradeoff among low-complexity detection algorithm for MIMO-LTE receivers," International Journal of Commun. Systems, Vol. 22, No. 7, pp. 885-897, July 2009.